Proceedings of the 20th International Conference on Soil Mechanics and Geotechnical Engineering– Rahman and Jaksa (Eds)

Embedded walls as a measure to mitigate the ground deformations at Section 63 of Lisbon Metro, Portugal

Paroi moulée comme mesure pour atténuer les déformations du sol à la Section 63 du Métro de Lisbonne, Portugal

António M.G. Pedro
ISISE, Department of Civil Engineering, University of Coimbra, Portugal, amgpedro@dec.uc.pt

José C.D. Grazina & David W. Massicano
Department of Civil Engineering, University of Coimbra, Portugal

ABSTRACT: It is widely known that the construction of shallow tunnels induces ground deformations that can cause severe damage to nearby buildings. A solution that can be adopted to mitigate the ground deformations consists in the pre-construction of an embedded wall between the tunnel and the buildings. Having as reference the case of the Section 63 of the Lisbon Metro, Portugal, this paper assesses what could have been the impact of using an embedded wall to mitigate the settlements induced by the construction of the running tunnel, which occurred in challenging hydrogeological ground conditions. After the calibration of the numerical model based on the back-analysis of the settlements that occurred in Section 63, the embedded wall is introduced in the model and its impact is assessed for different distances and depths of the wall. Based on the results it is possible to conclude about the importance of the hydrogeological ground conditions, which, in this particular case, condition the efficiency of using this type of solution. As expected, a significant reduction of the ground deformations is observed with the increase of the embedment depth of the wall and with its proximity to the tunnel.

RÉSUMÉ : Il est bien connu que la construction de tunnels peu profonds induit des déformations du sol qui peuvent causer de graves dommages aux bâtiments voisins. Une solution qui peut être adopté pour atténuer les déformations du sol consiste en la pré-construction d'une paroi moulée entre le tunnel et les bâtiments. Ayant comme référence le cas de la Section 63 du métro de Lisbonne, Portugal, cet article évalue ce qui aurait pu être l'impact de l'utilisation d'une paroi moulée pour atténuer les tassements induits par la construction du tunnel, qui a été excavé dans un défi hydrogéologique les conditions du sol. Après l'étalonnage du modèle numérique basé sur l'analyse rétrospective des tassements survenus à la section 63, la paroi moulée est introduite dans le modèle et son impact est évalué pour différentes distances et profondeurs encastré. Sur la base des résultats, il est possible de conclure sur l'importance des conditions hydrogéologiques du sol qui, dans ce cas particulier, conditionnent l'efficacité de l'utilisation de ce type de solution. Comme prévu, une réduction significative des déformations du sol est observée avec l'augmentation de la profondeur d'enfoncement de la paroi et avec sa proximité du tunnel.

KEYWORDS: Embedded wall, tunnelling, ground deformations, numerical analysis.

1 INTRODUCTION

The increase of population in big city centres resulted in a higher demand for effective transportation networks. In this context, tunnelling has proved to be an ideal solution since it increases considerably the safety and efficiency of the traffic flow, while it frees up land at the ground surface for other uses (Admiraal & Cornaro, 2016).

However, tunnelling can induce significant movements on the ground surface, which can damage structures located nearby, and therefore a detailed analysis of the impact of its construction must be performed (Mair, 2008). Regardless of the tunnelling method employed, it is almost impossible to excavate a tunnel without avoiding the decompression of the surrounding soil. Unavoidably, this stress relief induces displacements towards the tunnel perimeter and face, and, as a result, a deformation appears at the ground surface, which is usually termed as "settlement trough". The volume of the settlement trough, which corresponds to the ground volume excavated in excess, is known as "Volume Loss" (V_s), and for simplicity of interpretation it is usually expressed as a percentage of the excavated volume of the tunnel.

In order to mitigate the magnitude of these movements and minimise their detrimental effects on structures several protection techniques have been developed and employed (Harris, 2001). According with Burland (1995) before implementing any ground surface technique the protective measures should be applied within the tunnel, as these directly reduce the soil decompression and are generally less expensive. Measures typically employed within the tunnel may include: the strengthening of the support at or near the tunnel face; faster application of the support; decrease of the unsupported length; application of sprayed concrete linings; and/or dividing the excavation of the full section into smaller sections (Harris, 2001).

Nevertheless, in the case of buildings that require specific protection, due to their position in relation to the tunnel, Burland (1995) suggested the use of other alternative protection measures, such as the described below:

- Ground improvement: this technique aims to reduce ground loss by improving the mechanical properties of the soil near the tunnel or underneath the structure foundations with grout injections, compaction or drainage (Nicolini & Nova, 2000; Quick et al., 2001).
- Compensation grouting: the principle of the technique is to inject grout between the building's foundation and the tunnel to fill the soil voids and compensate for any ground movement induced by tunnelling (Lee, 2002; Zhang et al., 2013).
- Structural strengthening: this category comprises all the actions applied on the structures with the aim of stiffening or strengthening them. This can be achieved by the installation of new reinforcing elements, by modifying the foundation system or by installing jacks which can control the foundations movements (Frischmann et al., 1994; de Urríes et al., 2002).
- Physical Barrier: the installation of a physical barrier between the tunnel and the building may be capable of changing the shape of the settlement trough by reducing the settlements behind the wall (Bai et al., 2014; Ledesma & Alonso, 2017).

This last technique is particularly employed in cases where improving the ground conditions is difficult and it would require

a significant cost. Several types of embedded walls, such as a continuous line of bored piles (Bai et al., 2014; Ledesma & Alonso, 2017), jet-grouting columns (Sola et al., 2003) and micropiles (Nikiforova & Vnukov, 2011), have been employed. In all these cases it was observed that this technique significantly reduced the ground movements on the footprints of the buildings and, consequently, the potential damage on them, making it reliable. However, and despite the practical evidence, the design of embedded walls is often based on empiricism, rather than on a rational process (Rampello et al., 2019). Only more recently, the studies performed by Bilotta (2008), Rampello et al. (2019) and Massicano (2020) presented a detailed literature review, supported by experimental and numerical results, that explain in detail the interaction between the embedded wall and the soil. In general terms, all studies concluded that the offset distance of the barrier to the tunnel centreline and the height of the embedded wall were very important parameters, although no optimal values were suggested as they varied with the geometrical and ground conditions analysed. In contrast, parameters such as the wall stiffness and roughness appear to have a minimal effect on the efficiency of the barrier.

In order to determine the embedded wall's efficiency in reducing the settlements behind the wall, Bilotta (2008) used a dimensionless ratio, η_l, given by Equation 1, termed as local efficiency. In the equation, $\delta_{v,w}$ is the settlement immediately behind the top of the wall, while $\delta_{v,ref}$ is the settlement in greenfield conditions, i.e., without barrier, at the same location.

$$\eta_l = 1 - \frac{\delta_{v,w}}{\delta_{v,ref}} \quad (1)$$

As defined by the equation a $\eta_l = 1$ implies a total efficiency of the embedded wall since $\delta_{v,w} = 0$. On the other hand, the embedded wall is considered completely ineffective if $\eta_l = 0$, as $\delta_{v,w} = \delta_{v,ref}$. In the case of $\eta_l < 0$ the effect of the embedded wall is detrimental (Bilotta, 2008). Since this ratio only relies on the settlement observed immediately behind the top of the wall Rampello et al. (2019) suggested the use of a more global indicator and proposed the use of Equation 2, which is defined in terms of volume loss and defines the global efficiency of the wall (η_g).

$$\eta_g = 1 - \frac{V_{s,w}}{V_{s,ref}} \quad (2)$$

In the equation $V_{s,w}$ is the volume of the settlement trough (expressed as a percentage of the excavated volume of the tunnel) with the wall installed and $V_{s,ref}$ is the volume of the settlement trough in greenfield conditions. Also in this case η_g value has an equivalent meaning to that described for η_l. Massicano (2020) suggested that for clarity the global efficiency should be separated into two parcels, one corresponding to the volume behind the wall ($\eta_{g,be}$) and the other to the volume in front of the wall ($\eta_{g,fr}$)), which includes the location of the tunnel, since the influence on the volume is completely different on each side of the wall.

Based on these concepts this work presents the case of Section 63 of the Lisbon metro network (Green Line), Portugal, where the monitoring results showed significant settlements during the tunnel excavation. In order to evaluate what could have been the impact of using an embedded wall in the mitigation of those settlements an extensive numerical analysis was performed. After the calibration of the model a parametric study is carried out for assessing the optimal position and height of the embedded wall. The influence of the challenging hydrogeological and stratigraphic local ground conditions is also evaluated by performing some additional analyses.

2 SECTION 63 OF THE LISBON METRO NETWORK

2.1 *Location and geometry*

The growth of Lisbon, Portugal, at the end of the 19th century resulted in a lack of available and affordable land and triggered the idea of constructing a metro network. The works only started after the 2nd World War, but since then several expansions have been performed and others are planned for the nearby future. Section 63 of the Lisbon metro network is about 600 m long and is located on the Green Line, between the "Cais do Sodré" and the "Baixa-Chiado" stations, connecting the riverside area to one of the several hills of the city and standing right bellow some World Heritage buildings and very degraded structures in a massively dense area of Lisbon (Figure 1).

Its construction started in the second semester of 1994 using an EPB-TBM (Salgueiro Amaral, 2006), with the excavation process beginning at the "Cais do Sodré" station towards the "Baixa-Chiado" station. The alignment of Section 63 is curved, with a maximum radius of 170 m, and has a maximum slope of 4%, with its cover in the initial part varying from 9.5 m to 13.5 m. The running tunnel has a circular section with an external diameter, D_t, of 9.7 m, supported by 0.36 m thick and 1.2 m long precast concrete segments (Salgueiro Amaral, 2006). Between 0+200 m and 0+500 m of Section 63 several cross-sections were instrumented, with cross-section P10A (0+350 m) being of particular interest to this paper (Figure 1).

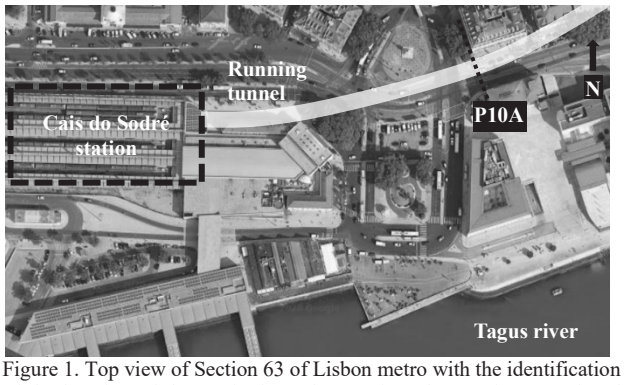

Figure 1. Top view of Section 63 of Lisbon metro with the identification of the location of the "Cais do Sodré" station, the running tunnel and cross-section P10A.

2.2 *Geological conditions*

The profile showing the stratigraphy at the instrumented cross-section P10A is depicted in Figure 2. The ground conditions at this location of Lisbon are very complex and influenced by the Tagus river, which is at a distance of about 100 m on the south side (Figure 1). The deepest formations, Areolas da Estefânia" (AE) and "Argilas dos Prazeres" (AP), are part of the Miocene deposits, which were deposited in a marine-continental environment around 24 million years ago (Moitinho de Almeida, 2008). After, due to some tectonic events and influenced by the Tagus basin location, the formations bended towards the Tagus river. A subsequent sea regression exposed the layers, which suffered a period of intense erosion, which was then followed by a new sedimentation process, where the more superficial Alluvium layer was deposited. The current geological profile was finally defined after the deposition of a layer of Fill, with about 6m thick, which had the purpose of reclaim land to the Tagus basin and achieve a solid platform for construction. The water level is located at approximately 1.2 m depth.

At cross-section P10A the centre of the tunnel is located at about 16.3 m depth and its section coincides with the transition between the Miocene formations, with the major excavation occurring on the AE formation, while the AP formation appears mainly at the bottom and left-hand side. This asymmetry is aggravated by the distinct nature of the Miocene formations, as

the AE formation is mainly constituted by sand and silt and the AP formation is composed of clay. This implies that beside the different mechanical characteristics there is a complete contrast in terms of hydrogeological behaviour, which made extremely difficult to control the face pressure applied during the excavation by the EPB-TBM.

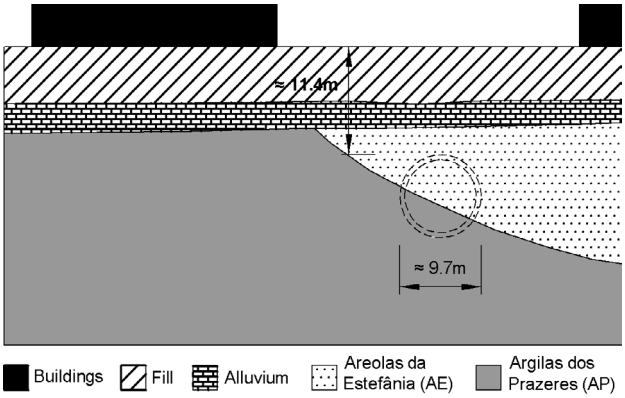

Figure 2. Geological profile of the cross-section P10A (adapted from Salgueiro Amaral (2006)).

2.3 *Instrumentation results*

Giving the challenging conditions observed at Section 63 of Lisbon metro it was decided to implement a rigorous instrumentation plan to measure the surface ground movements in the tunnel vicinity. This plan allowed monitoring the integrity of the adjacent buildings and to careful control the face pressure of the EPB-TBM (Salgueiro Amaral, 2006). A total of 10 cross-sections were defined and instrumented with settlement sensors, extensometers, inclinometers and piezometers.

The results in almost all sections revealed an asymmetric settlement trough, which was in line with the asymmetric stratigraphy of the ground, showing higher movements on the side where the Tagus river is located. The first cross-sections, near the "Cais do Sodré" station, were excavated under the protection of jet-grouting columns and presented small settlements ($\delta_{max} = 6.5\ mm$). However, and despite the use of compensation grouting in most of the alignment, the settlements increased significantly as the excavation moved away from the station, reaching a maximum value at cross-section P9 (0+300) of 66.9 mm. In order to control and reduce the deformations the EPB-TBM face pressure was gradually increased (Salgueiro Amaral, 2006). As a result, in cross-section P10A a smaller settlement of 36.4mm was measured while in the following cross-sections the values continued to reduce and stabilized at about 15 mm. As the excavation moved towards "Baixa-Chiado" station the cover increased considerably and the ground conditions improved with the tunnel section being fully excavated at the stiffer AP formation, which made the excavation less demanding. After the conclusion of the works most of the instrumentation was removed and no information concerning the long-term settlements is available in the literature.

3 NUMERICAL MODEL

In order to evaluate the influence of using an embedded wall in the mitigation of the settlements observed at Section 63 an extensive numerical 2D analysis was performed using RS2 software. Plane strain conditions were assumed with the domain discretized into 6-noded triangles finite continuum elements. To properly simulate the ground conditions and the changes observed in the water level due to the excavation of the tunnel a coupled consolidation analysis was performed. The study had as reference cross-section P10A (Figure 2), since the results in this section showed a more typical behaviour, which was not significantly affected by the lack of control of the face pressure applied by the EPB-TBM or by the effects of the compensation grouting.

Figure 3 illustrates the 2D model employed, which has 150 m width and a height of 33.2 m, with the tunnel centred in the model. The stratigraphy is similar to that presented in Figure 2, apart from the Fill and the Alluvium layer, which were merged into a single layer (AL) since the parameters available in the literature were identical to both of them. Beside the greenfield analysis, where no embedded wall was considered, a total of 20 configurations were analysed. Those corresponded to five offset distances of the embedded wall to the tunnel centreline (d/Dt = 0.75; 1.00; 1.25; 2.00 and 3.00), varying from an extreme distance of just 2.4 m (d/Dt = 0.75) to about 24.3 m (d/Dt = 3.00) away from the sidewall of the tunnel. In terms of height of the wall four cases were considered, with the tip being located at the depth of the crown (h/Dt = -0.50), at its centre (h/Dt = 0.00), at the bottom (h/Dt = 0.50) and half a diameter below the tunnel (h/Dt = 1.00). In all cases it was decided to place the embedded wall on the side of the Tagus river, since the ground conditions were poorer on that side and higher movements were expected. It should also be noted that due to the stratigraphy in some of the scenarios the tip of the wall was embedded in the AP layer, which modified significantly both the seepage and the foundation of the wall conditions.

The parameters adopted for the three layers are presented in Table 1 and had as reference the studies of Mateus de Brito & Matos Fernandes (2006), Pedro (2013) and Ferreira et al. (2018). In all cases an elastic-perfectly-plastic constitutive model with a Mohr-Coulomb failure criterion was adopted. The lining of the tunnel and the embedded wall were simulated using beam elements. A linear elastic behaviour with a Young's modulus of 30 GPa and a Poisson's coefficient of 0.2 was adopted for both, with the only difference being the thickness, which was 0.36 m for the lining and 0.6 m for the wall. An interface between the embedded wall and the soil with mechanical parameters equal to 2/3 of the adjacent soil layer was also considered in the analyses.

Table 1. Properties adopted for the soil layers.

Formation		AL	AE	AP
γ	(kN/m^3)	18	20	20
K_0	(-)	0.5	0.7	0.7
c'	(kPa)	0	4	50
ϕ'	(º)	33	42	35
ψ	(º)	0	0	0
E'$_s$	(MPa)	10	38.5	435
ν	(-)	0.3	0.3	0.3
k	(m/s)	1×10^{-9}	1×10^{-5}	1×10^{-9}

The construction sequence adopted in both greenfield and embedded wall analyses consisted of three stages. The initial stage comprised the generation of a geostatic stress state using the unit weights (γ) and earth pressure coefficients (K_0) presented in Table 1. When present, it was assumed that the embedded wall was already in place in the first stage and, consequently, any effects caused by its installation were not considered in the analyses. The 3D effects related to the excavation of the tunnel were introduced in the 2D analyses following the principles of the convergence-confinement method (Potts & Zdravković, 2001). Consequently, in the second stage the elements inside the tunnel were removed but only part of the released forces, corresponding to a stress release factor, α, were applied in the excavation contour. In the third and final stage the lining of the

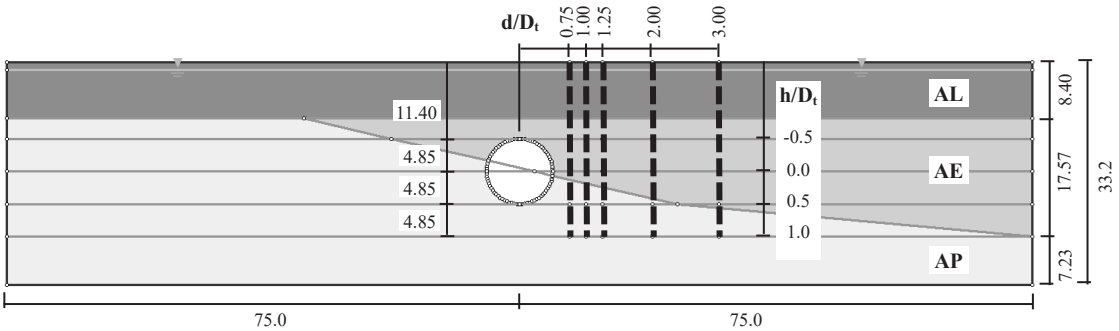

Figure 3. Numerical model with the different positions of the embedded walls considered in the analyses.

tunnel was installed, and the remainder unbalanced forces (1-α) applied, so that a final state of equilibrium was reached.

In respect to the displacement boundary conditions, a "free surface" was considered on top, rollers on the lateral sides (restrained in the horizontal direction) and pinned on the bottom of the model. As for the hydraulic boundary conditions an initial piezometric level at 1.2 m depth was considered in all stages on both sides of the model, implying that there was throughout the analysis a constant and permanent flow. To simulate the partial drainage that occurred due to the excavation of the tunnel it was considered in the second stage a reduction of the total head in the entire contour of the tunnel, which was calibrated to be equal to that caused by the soil removal. Consequently, that implied that an equal stress relief factor was considered for both stress and hydraulic conditions. Since the tunnel was meant to be impermeable after the installation of the lining, and the only concern was to simulate the short-term behaviour, it was decided in the final stage to maintain the hydraulic conditions in the contour of the tunnel as defined in the second stage, ensuring that the water conditions modified by the excavation remained unchanged. Finally, it should be noted that when present the embedded wall was considered to be impermeable.

After the definition of the construction sequence and of the appropriate boundary conditions the parameter α was calibrated so that in the final stage the maximum settlement determined in the greenfield analysis was equal to that measured by the instrumentation at cross-section P10A (36.4 mm). After a trial-and-error approach a stress release factor α = 0.58 was determined, which corresponded to a reference volume loss of $V_{s,ref} = 2.22\%$.

4 EFFICIENCY OF THE EMBEDDED WALL

Figure 4 presents the settlement troughs obtained for the greenfield analysis and for the cases where the embedded wall was located at the bottom of the tunnel (h/Dt = 0.5) for the different offset distances considered. In accordance with the instrumentation results the greenfield analysis shows an asymmetric behaviour with higher displacements on the side of the AE formation. This is due to the softer nature of this layer and also to the hydrological conditions, since the higher permeability of this layer increases considerable the seepage on that side. In contrast, on the AP formation side there is almost no seepage due to the low permeability of this formation, with the curve exhibiting a more typical behaviour.

The influence of the embedded wall in restraining the settlements is evident in all analysis. Naturally, the effect of the wall is gradually higher with its proximity to the tunnel. The wall introduces a discontinuity on the settlement trough with the results in front of it being similar in all cases. However, behind the wall it is possible to observe a significant reduction of the volume loss, particularly for offset distances smaller than d/Dt < 2.00. The global efficiency obtained for each of the 20 configurations of the embedded wall analysed is presented in

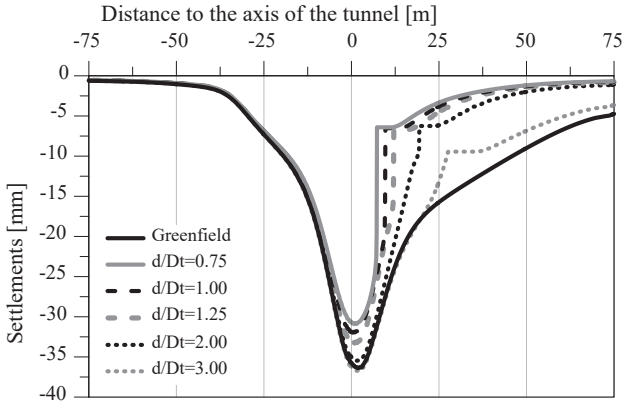

Figure 4. Settlement troughs for the greenfield and for the analyzed offset distances of the wall for an embedment depth of h/Dt = 0.5.

Figure 5. To facilitate the interpretation the cases where the wall was embedded in the AP formation were identified with solid symbols. The results show a significant influence of the embedment of the wall, with the global efficiency increasing substantially when the wall was founded in the AP formation. This result is justified due to the higher stiffness and strength of this layer but also because of its low permeability, which makes seepage more difficult. The global efficiency is almost identical for the cases where the wall is extended to depths of h/Dt = 0.5 and 1.0 up to an offset distance of d/Dt = 2.0. From this point there is a difference with the h/Dt = 0.5 analysis showing a decrease of efficiency of nearly 50% (0.2 vs 0.1) for d/Dt = 3.0, which is justified by the lack of embedment on the AP formation. For the cases where the height of the wall is smaller (h/Dt = -0.5 and h/Dt = 0.0) the global efficiency is reduced not surpassing 0.11. In fact, it is possible to observe that for the case where the wall is placed at the crown of the tunnel level (h/Dt = -0.5) its presence is completely irrelevant, regardless of the offset distance considered. As shown in Figure 4, the results reveal a significant increase of the global efficiency of the wall with its proximity to the tunnel for the cases where a deeper wall is considered, with a value of about 0.5 obtained for d/Dt = 0.75. It is also interesting to note that this trend is not observed for the shortest walls where a decrease of global efficiency is observed for d/Dt = 0.75. This behaviour is caused by the proximity of the tip of the wall to the tunnel, which causes a stress concentration in the area leading to an increase of the soil plastification.

As suggested by Massicano (2020) the results of the global efficiency were separated into the behind ($\eta_{g,be}$) and front ($\eta_{g,fr}$) of the wall components, with the results obtained for the h/Dt = 0.5 scenario depicted in Figure 6. As the previous results suggested the figure clearly shows that the global efficiency of the wall is mainly achieved by the reduction of the volume loss behind the wall. This component corresponds to about 85% of the total value, regardless of the offset distance considered. It should also be mentioned that the remainder 15% occur essentially in the distance between the wall and the opposite

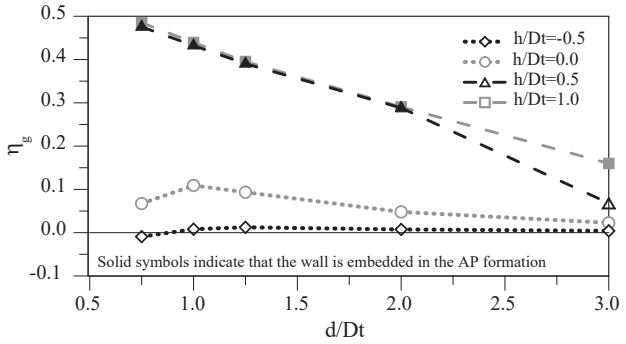

Figure 5. Global efficiency for the analyzed offset distances of the wall

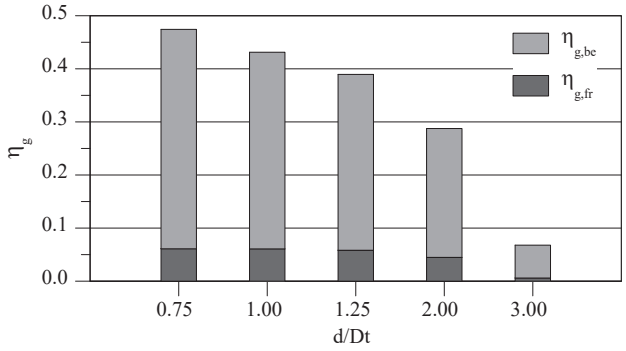

Figure 6. Global efficiency distribution behind and in front of the wall for an embedded wall with a h/Dt = 0.5.

sidewall of the tunnel (Figure 4), being completely insignificant beyond that location. A similar behaviour, with identical distribution was obtained for the other heights of the wall analysed.

The local efficiency, computed based on the displacements immediately behind the top of the wall, is presented in Figure 7. The analysis was performed not just for the settlements, as proposed by Bilotta (2008), but also for the horizontal displacements (using horizontal displacements in Equation 1). As previously, the solid symbols indicate cases where the wall is embedded in the AP formation. In terms of settlements the results of the local efficiency show an almost identical behaviour when compared with that observed for the global efficiency, being only higher in magnitude. Also in this case the embedment of the wall in the AP formation has a fundamental effect. To the depth of h/Dt = 1.0, where the wall is always founded in the AP formation, the local efficiency is very high, decreasing from just 0.80 to 0.65 as the offset distance to the tunnel (d/Dt) increases from 0.75 to 3.00. The positive effect of the wall is also very relevant for a depth of h/Dt = 0.5 and even for the highest offset distance considered (d/Dt = 3.00) a local efficiency of about 40% is achieved, despite the lack of embedment of the wall in this scenario. Even for the shortest walls, which are not founded in the AP formation, there is still a relevant effect, which tends to decrease with the increase of the offset distance and with the decrease of the height of the wall. As observed for the global efficiency it is also noticeable for the closest and shortest walls a detrimental effect caused by the proximity of the tip of the wall to the tunnel.

The results of the local efficiency defined in terms of horizontal displacements are more complex. For offset distances d/Dt ≤ 1.00 a positive effect can be observed, which is essentially justified by the increase of stiffness induced by the wall, which restrains the horizontal movements. For higher offset distances a distinction must be made depending on the height of the wall. For shorter walls (h/Dt ≤ 0.00) there is almost no impact caused by the installation of the wall, with a local efficiency of about zero. However, for deeper walls a relevant detrimental effect is

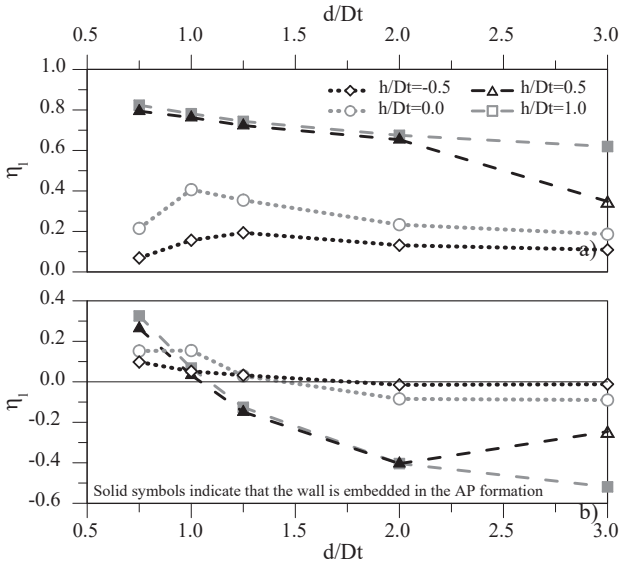

Figure 7. Local efficiency for the analyzed offset distances of the wall: a) settlements; b) horizontal displacements.

observed, which is clearly caused by the embedment of the wall in the AP formation. In those scenarios the natural flow of the water towards the tunnel is significantly restrained by the wall, causing an increase of the hydraulic pressures on it, which is reflected on the higher values of the horizontal displacements. As expected, as the offset distance increases and the wall remains embedded, the local efficiency decreases since the reference horizontal displacements in greenfield conditions are smaller. It is also interesting to note that for the d/Dt = 3.00 and h/Dt ≤ 0.50 case, where no embedment in the AP formation exists, a sharp reduction of the detrimental effect is observed, which is still about -0.25 but smaller than -0.40, which was the minimum observed when embedment occurred.

5 INFLUENCE OF THE GROUNDWATER CONDITIONS

In order to evaluate the influence of the embedment wall in the AP formation on the groundwater conditions a set of additional analyses was performed for a wall with a depth of h/Dt = 0.50. In these analyses the permeability of the AP formation was considered equal to that of the AE formation ($1x10^{-5}$ m/s) with all the other parameters and conditions remaining unchanged. With the change of permeability, the hydraulic conditions in the model become symmetrical and no additional obstacle in the seepage is induced by the embedment in the AP layer.

The results of the global and local efficiencies are presented in Figure 8 for both the previous (k-variable) and additional (k-constant) analyses. Overall, all trends observed remain identical and only the magnitude of the results was modified. On both global and local efficiency in terms of settlements a significant decrease of efficiency (which reaches more than 100%) is observed when a constant permeability is employed. This reduction tends to decrease with the offset distance and for the highest value considered (d/Dt = 3.00) the values of both analyses are identical, which was expected, since no AP embedded already existed in the reference analysis. These results clearly demonstrate the importance of restraining the water flow on the volume loss and on the settlements. In opposition, the local efficiency in terms of horizontal displacements exhibits a considerable increase, which originates a positive effect of the wall for offset distances of about d/Dt < 2.0. The increase on efficiency of nearly 300% is approximately equal for all offset distances, apart from the highest distance, where, once again, the results of both analyses converge.

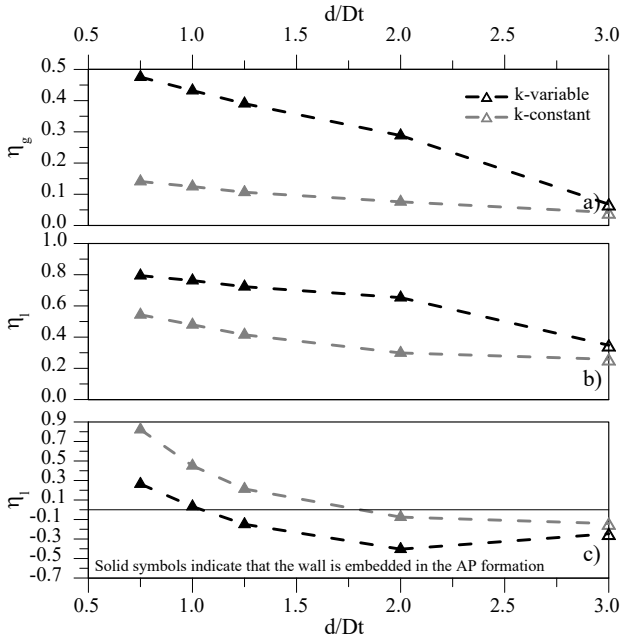

Figure 8. Influence of the groundwater conditions for an embedded wall with a h/Dt = 0.5: a) global efficiency; b) local efficiency – settlements; c) local efficiency – horizontal displacements.

6 CONCLUSIONS

This paper presents the case study of Section 63 of Lisbon Metro, Portugal, where significant settlements were observed during the excavation of the running tunnel due to the challenging hydrogeological ground conditions. In order to investigate if the installation of an embedded wall could mitigate the ground movements an extensive numerical analysis was performed, based on which the following conclusions can be drawn.

- Walls shorter than the centre level of tunnel (h/Dt ≤ 1.00) have a reduced efficiency, regardless of its offset distance to the tunnel, and, consequently, are not recommended.

- For deeper walls (h/Dt ≥ 0.50), the key factor is the embedment in the AP formation since it restrains the water flow towards the excavation and influence significantly both global and local efficiencies.

- Global efficiency increases considerably with the proximity of the wall to the tunnel for deeper walls (particularly for d/Dt ≤ 1.25), with the highest component being the reduction of the volume loss behind the wall, which is responsible for about 85% of the total reduction. A similar trend on deeper walls is observed for the local efficiency in terms of settlements, with the magnitude being even higher for all offset distances.

- A complete opposite effect is observed in the local efficiency in terms of horizontal displacements where the installation of the wall has a detrimental effect for d/Dt ≥ 1.25, due to the embedment in the AP formation, which restrained the water flow and caused higher pressures on the wall.

- The constant permeability analyses confirmed about the influence of the wall embedment in the AP formation on the water flow, with a significant reduction of efficiency observed if no embedment existed and the water flow was not restrained.

7 REFERENCES

Admiraal, H. & Cornaro, A. (2016) Why underground space should be included in urban planning policy – And how this will enhance an urban underground future. *Tunnelling and Underground Space Technology*, **55** pp. 214-220. https://doi.org/10.1016/j.tust.2015.11.013

Bai, Y., Yang, Z. & Jiang, Z. (2014) Key protection techniques adopted and analysis of influence on adjacent buildings due to the Bund Tunnel construction. *Tunnelling and Underground Space Technology*, **41** pp. 24-34. https://doi.org/https://doi.org/10.1016/j.tust.2013.11.005

Bilotta, E. (2008) Use of diaphragm walls to mitigate ground movements induced by tunnelling. *Géotechnique*, **58** (2), pp. 143-155. https://doi.org/10.1680/geot.2008.58.2.143

Burland, J. B. (1995) Assessment of risk of damage to buildings due to tunnelling and excavation. In *Proceedings of the 1st International conference on earthquake geotechnical engineering, IS Tokyo '95.* Ishihara, K. (ed.), Vol. 3, pp. 1189-1201.

de Urríes, M. F. J., Crespo, A. S., del Monte Ramos, E. & Rodríguez, P. R. (2002) The Excavation of a Shallow Tunnel Below a Commercial Centre. In *Proceedings of the GAUCSG, Third International Symposium (Toulouse, France)*, pp. 47-52.

Ferreira, T., Pedro, A. M. G. & Almeida e Sousa, J. (2018) Evaluation of the Hardening soil model's ability to reproduce the soil response to different loading conditions. In *Proceedings of the XVI National Conference in Geotechnics, S. Miguel, Azores, Portugal.* pp. 12 (in Portuguese).

Frischmann, W., Hellings, J., Gittoes, G., Snowden, C. & DLR (1994) Protection of the Mansion House against damage caused by ground movements due to the Docklands Light Railway extension. *Proceedings of the Institution of Civil Engineers-Geotechnical Engineering*, **107** (2), pp. 65-76

Harris, D. I. (2001) "*11 Protective measures*" *Building response to tunnelling*, CIRIA, pp. 135-176.

Ledesma, A. & Alonso, E. E. (2017) Protecting sensitive constructions from tunnelling: the case of World Heritage buildings in Barcelona. *Géotechnique*, **67** (10), pp. 914-925. https://doi.org/10.1680/jgeot.SiP17.P.155

Lee, S. W. (2002) The use of compensation grouting in tunnelling: a case study. *Proceedings of the Institution of Civil Engineers-Geotechnical Engineering*, **155** (2), pp. 101-109

Mair, R. J. (2008) Tunnelling and geotechnics: new horizons. *Géotechnique*, **58** (1), pp. 695-736

Massicano, D. (2020) *Assessment of the Efficiency of Embedded Walls to Mitigate Ground Deformations Induced By Tunnelling*. MSc Thesis. University of Coimbra, Coimbra, Portugal.

Mateus de Brito, J. M. & Matos Fernandes, M. (2006) Estação Terreiro do Paço do Metropolitano de Lisboa: concepção, previsões de projecto e desempenho. In *Proceedings of the III Congresso Luso-Brasileiro de Geotecnia, Lisboa, Portugal.* pp. 21-42 (in Portuguese).

Moitinho de Almeida, I. (2008) In *Guia de Telheiras*, Lisbon, pp. 4. (in Portuguese).

Nicolini, E. & Nova, R. (2000) Modelling of a tunnel excavation in a non-cohesive soil improved with cement mix injections. *Computers and Geotechnics*, **27** (4), pp. 249-272. https://doi.org/10.1016/S0266-352x(00)00003-3

Nikiforova, N. & Vnukov, D. (2011) Geotechnical cut-off diaphragms for built-up area protection in urban underground development. In *Proceedings of the The proc. of the 7th Int. Symp. of Geotechnical aspects of underground construction in soft grouning*, Vol. 18.

Pedro, A. M. G. (2013) *Geotechnical investigation of Ivens shaft in Lisbon*. PhD Thesis. Imperial College London, London, UK.

Potts, D. M. & Zdravković, L. (2001) *Finite element analysis in geotechnical engineering: application.* Thomas Telford. London.

Quick, H., Michael, J. & Arslan, U. (2001) About the effect of preliminary measures on ground movements due to tunnelling. *Response of Building to Excavation-Induced Ground Movements, London*, **17** pp. 18

Rampello, S., Fantera, L. & Masini, L. (2019) Efficiency of embedded barriers to mitigate tunnelling effects. *Tunnelling and Underground Space Technology*, **89** pp. 109-124. https://doi.org/https://doi.org/10.1016/j.tust.2019.03.027

Salgueiro Amaral, M. J. (2006) *Analysis of the observation results from Lisbon Metropolitan tunnels*. Master's thesis. University of Oporto, Oporto (in Portuguese).

Sola, P. R., Monroe, A. S., Martin, L., Blanco, M. A. & San Juan, R. (2003) "*Ground treatment for tunnel construction on the Madrid Metro*" *Grouting and Ground Treatment*, pp. 1518-1533.

Zhang, D., Fang, Q., Hou, Y., Li, P. & Yuen Wong, L. N. (2013) Protecti on of Buildings against Damages as a Result of Adjacent Large-Span Tunneling in Shallowly Buried Soft Ground. *Journal of Geote chnical and Geoenvironmental Engineering*, **139** (6), pp. 903-913. https://doi.org/10.1061/(asce)gt.1943-5606.0000823